Three-phase Inductive Power Transfer System with 12 coils for Radiation Noise Reduction

Keisuke Kusaka[1*] and Jun-ichi Itoh[2]
1 Department of Electrical, Electronics and Information Engineering, Nagaoka University of Technology, Nagaoka, Japan
2 Department of Science of Technology Innovation, Nagaoka University of Technology, Nagaoka, Japan

*E-mail: kusaka@vos.nagaokaut.ac.jp

***Abstract*— A three-phase inductive power transfer system with six transmission coils and six receiving coils is proposed in this paper. The proposed system achieves a reduction in radiation noise by canceling the noise using multiple coils, which are placed opposite to each other. However, in IPT systems with multiple coils, a magnetic interference among the multiple coils decreases a transmission efficiency due to the occurrence of circulating current. The proposed three-phase IPT system achieves cancellation of the interference using six coils on each side. First, the IPT system with the 12 coils is proposed. Then, a canceling condition of the magnetic interference among the coils is mathematically introduced from the voltage equation on the coils. Finally, the proposed IPT system is experimentally demonstrated with the 3-kW prototype. The experimental result shows that the radiation noise at the fundamental frequency is suppressed to 1/6 (from 12.2dBμA to 2.1dBμA).**

Keywords*— inductive power transfer, wireless power transfer, three-phase transmission

I. INTRODUCTION

In recent years, inductive power transfer (IPT) systems for electrical vehicles (EVs) are actively studied [1–11] because IPT systems are capable of improving the usability of EV users. In order to put the IPT system for practical use, a standardization of the IPT system for EVs is ongoing [12–13]. According to the standards, which will be published by IEC/ISO, the IPT systems will be classified by the maximum input power into four class; the maximum input power is ≤ 3.7 kW for WPT1, the maximum input power is > 3.7 kW and ≤ 7.7 kW for WPT2, the maximum input power is > 7.7 kW and ≤ 11 kW for WPT3, the maximum input power is > 11 kW and ≤ 22 kW for WPT4, and the maximum input power is > 22 kW for WPT5 [12–13].

The standardization of WPT1 and WPT2 are currently in progress. However, the standardization of high-power IPT systems such as WPT5 has not been discussed well despite strong demand for higher power IPT system for heavy-duty vehicles because high-power IPT systems may cause two problems. One of the problems is a decrease in transmission efficiency. Copper loss and iron loss on transmission coils may increase because the current in the transmission coils increases [14]. The second problem is radiation noise. The radiation noise caused by the IPT systems must satisfy the regulations, which are published by CISPR or legislated in each country or region. However, the satisfaction of regulations becomes further difficult because the radiation noise caused by a loop coil is proportional to the conduction current.

In previous studies, a radiation noise reduction technique using a duplicated 44-kW IPT system for heavy-duty EVs has been proposed [14–16]. In [15], the radiation noise is canceled by duplicated transmission coils. The two transmission coils with differential current are placed to cancel out the leakage radiation noise. However, the duplicated IPT system limits freedom of coil positions because the duplicated coils cause a magnetic interference between the duplicated coils [15]. The magnetic interference decreases power factor regarding an inverter output.

Meanwhile, three-phase IPT systems have been proposed to increase the output power of the IPT system [17-20]. The three-phase IPT systems allow the reduction of the current on each transmission coil. Thus the three-phase IPT is an effective method to reduce the copper loss and the iron loss. However, in the conventional three-phase IPT system, a magnetic interference among the additional coils on each side occurs. The magnetic interference causes a degrade the efficiency because the magnetic interference leads to circulating currents.

This paper proposes a three-phase IPT system with 12 solenoid coils, which consists of six pairs of coils placed opposite to each other. The proposed IPT system contributes reducing the current on the winding without a byproduct such as a magnetic interference. A contribution of this paper is offering the new transmission coil structure, which reduces the radiation noise with a small effect on efficiency. In the proposed system, the radiation noise is canceled out by the countercurrent in the opposite coil. Moreover, the primary coils and the secondary coils are placed at an angle of 60 degrees to each other. Consequently, the induced voltage caused by magnetic interference among

the 12 coils are canceled out. First, a system configuration of the proposed IPT system is unveiled. Next, a design procedure of the proposed three-phase IPT system with a star-star winding and a delta-delta winding is explained. Then, the canceling method of the magnetic interference among the multiple coils is mathematically introduced. Finally, the proposed IPT system with star-star winding is tested with a 3-kW prototype. Then, the radiation noise is assessed and compared between the conventional three-phase IPT system and the proposed three-phase IPT system with 12 coils.

II. THREE-PHASE IPT SYSTEM WITH 12 COILS

In this chapter, the three-phase IPT system is proposed. The proposed IPT system achieves radiation noise reduction using 12 coils without magnetic interference among multiple coils. In other words, the IPT system transmits power with unity power factor regarding inverter output.

A. System Configuration

Figure 1 shows the proposed three-phase IPT system with 12 coils. The three-phase coils can be connected with not only star-star winding but also star-delta, delta-star, and delta-delta windings. In this paper, only star-star and delta-delta windings are discussed due to the page limitation. Power is inductively transmitted through the three-phase coils. Each phase has two coils connected in series. These coils connected in series cancel out the radiation noise because of the countercurrent flowing on the coils [14].

Besides, the three-phase inverter in the primary side and the three-phase rectifier in the secondary side are used. The primary inverter output square-wave voltage in each phase. The phase difference of each phase are 120 degrees. Furthermore, resonant capacitors are connected to the output of the primary inverter and the input of the rectifier in series. The series-series compensation technique [21] is applied to the proposed system in order to cancel out the leakage inductance due to the weak magnetic coupling. Using three-phase IPT and the series-series compensation technique, copper loss of the windings can be reduced because the current is shunted into six coils. Therefore, the proposed IPT system is effective to improve the heat dissipation of the transmission coils.

Figure 2 shows the position and connection of the transmission coils. In the proposed IPT system, six solenoid coils are used in each of the primary side and the secondary side. Fig. 3 shows the mechanism of the reduction in radiation noise. Two transmission coils connected in series (e.g., L_{uv1A} and L_{uv1B}) are differentially connected and are placed in an opposite place. These opposite coils cancel out radiation noise at a measurement point, which is typically 10 m from the IPT system [22]. Other pairs of coils are placed in an angle of 120 degrees to the coils on phase-u each other. As a drawback of the reduction in radiation noise using opposite coils, magnetic interference occur among the six coils on each the primary side and the secondary side. In order to cancel out the magnetic interference, the position relationship and figure of the coils have to be adjusted. The design method of the coils will be explained in section C.

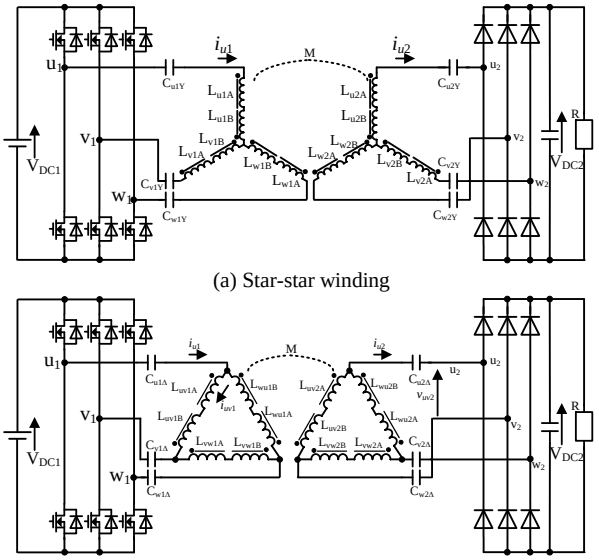

Fig. 1. Proposed three-phase IPT system with 12 coils.

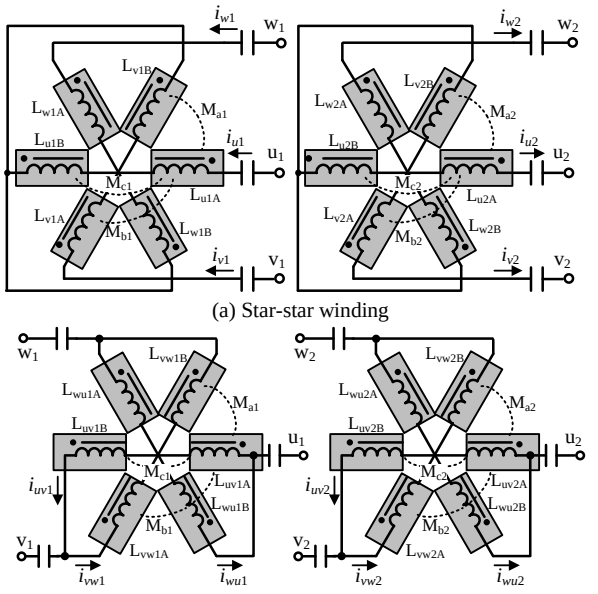

Fig. 2. Placement and connection of coils.

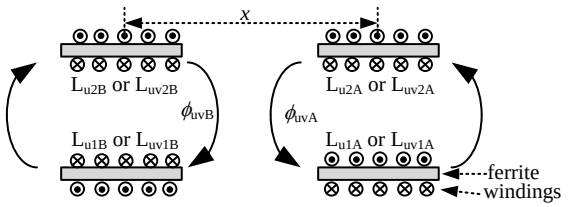

Fig. 3. Mechanism of reduction in radiation noise using solenoid coils.

B. Mathematical Expression of Three-phase Coils

Equations (1) and (2) represents the induced voltage of 12 coils on the star-star winding system and the delta-

$$\begin{pmatrix} v_{u1A} \\ v_{u1B} \\ v_{v1A} \\ v_{v1B} \\ v_{w1A} \\ v_{w1B} \\ v_{u2A} \\ v_{u2B} \\ v_{v2A} \\ v_{v2B} \\ v_{w2A} \\ v_{w2B} \end{pmatrix} = \begin{pmatrix} L_{1Ys} & M_{c1} & M_{b1} & M_{a1} & M_{b1} & M_{a1} & M & 0 & 0 & 0 & 0 & 0 \\ M_{c1} & L_{1Ys} & M_{a1} & M_{b1} & M_{a1} & M_{b1} & 0 & M & 0 & 0 & 0 & 0 \\ M_{b1} & M_{a1} & L_{1Ys} & M_{c1} & M_{b1} & M_{a1} & 0 & 0 & M & 0 & 0 & 0 \\ M_{a1} & M_{b1} & M_{c1} & L_{1Ys} & M_{a1} & M_{b1} & 0 & 0 & 0 & M & 0 & 0 \\ M_{b1} & M_{a1} & M_{b1} & M_{a1} & L_{1Ys} & M_{c1} & 0 & 0 & 0 & 0 & M & 0 \\ M_{a1} & M_{b1} & M_{a1} & M_{b1} & M_{c1} & L_{1Ys} & 0 & 0 & 0 & 0 & 0 & M \\ M & 0 & 0 & 0 & 0 & 0 & L_{2Ys} & M_{c2} & M_{b2} & M_{a2} & M_{b2} & M_{a2} \\ 0 & M & 0 & 0 & 0 & 0 & M_{c2} & L_{2Ys} & M_{a2} & M_{b2} & M_{a2} & M_{b2} \\ 0 & 0 & M & 0 & 0 & 0 & M_{b2} & M_{a2} & L_{2Ys} & M_{c2} & M_{b2} & M_{a2} \\ 0 & 0 & 0 & M & 0 & 0 & M_{a2} & M_{b2} & M_{c2} & L_{2Ys} & M_{a2} & M_{b2} \\ 0 & 0 & 0 & 0 & M & 0 & M_{b2} & M_{a2} & M_{b2} & M_{a2} & L_{2Ys} & M_{c2} \\ 0 & 0 & 0 & 0 & 0 & M & M_{a2} & M_{b2} & M_{a2} & M_{b2} & M_{c2} & L_{2Ys} \end{pmatrix} \frac{d}{dt} \begin{pmatrix} i_{u1} \\ -i_{u1} \\ i_{v1} \\ -i_{v1} \\ i_{w1} \\ -i_{w1} \\ i_{u2} \\ -i_{u2} \\ i_{v2} \\ -i_{v2} \\ i_{w2} \\ -i_{w2} \end{pmatrix} \tag{1}$$

$$\begin{pmatrix} v_{uv1A} \\ v_{uv1B} \\ v_{vw1A} \\ v_{vw1B} \\ v_{wu1A} \\ v_{wu1B} \\ v_{uv2A} \\ v_{uv2B} \\ v_{vw2A} \\ v_{vw2B} \\ v_{wu2A} \\ v_{wu2B} \end{pmatrix} = \begin{pmatrix} L_{1\Delta s} & M_{c1} & M_{b1} & M_{a1} & M_{b1} & M_{a1} & M & 0 & 0 & 0 & 0 & 0 \\ M_{c1} & L_{1\Delta s} & M_{a1} & M_{b1} & M_{a1} & M_{b1} & 0 & M & 0 & 0 & 0 & 0 \\ M_{b1} & M_{a1} & L_{1\Delta s} & M_{c1} & M_{b1} & M_{a1} & 0 & 0 & M & 0 & 0 & 0 \\ M_{a1} & M_{b1} & M_{c1} & L_{1\Delta s} & M_{a1} & M_{b1} & 0 & 0 & 0 & M & 0 & 0 \\ M_{b1} & M_{a1} & M_{b1} & M_{a1} & L_{1\Delta s} & M_{c1} & 0 & 0 & 0 & 0 & M & 0 \\ M_{a1} & M_{b1} & M_{a1} & M_{b1} & M_{c1} & L_{1\Delta s} & 0 & 0 & 0 & 0 & 0 & M \\ M & 0 & 0 & 0 & 0 & 0 & L_{2\Delta s} & M_{c2} & M_{b2} & M_{a2} & M_{b2} & M_{a2} \\ 0 & M & 0 & 0 & 0 & 0 & M_{c2} & L_{2\Delta s} & M_{a2} & M_{b2} & M_{a2} & M_{b2} \\ 0 & 0 & M & 0 & 0 & 0 & M_{b2} & M_{a2} & L_{2\Delta s} & M_{c2} & M_{b2} & M_{a2} \\ 0 & 0 & 0 & M & 0 & 0 & M_{a2} & M_{b2} & M_{c2} & L_{2\Delta s} & M_{a2} & M_{b2} \\ 0 & 0 & 0 & 0 & M & 0 & M_{b2} & M_{a2} & M_{b2} & M_{a2} & L_{2\Delta s} & M_{c2} \\ 0 & 0 & 0 & 0 & 0 & M & M_{a2} & M_{b2} & M_{a2} & M_{b2} & M_{c2} & L_{2\Delta s} \end{pmatrix} \frac{d}{dt} \begin{pmatrix} i_{uv1} \\ -i_{uv1} \\ i_{vw1} \\ -i_{vw1} \\ i_{wu1} \\ -i_{wu1} \\ i_{uv2} \\ -i_{uv2} \\ i_{vw2} \\ -i_{vw2} \\ i_{wu2} \\ -i_{wu2} \end{pmatrix} \tag{2}$$

delta winding system, respectively where L_{1Ys} is the self-inductance of each coil on the star-star winding, $L_{1\Delta s}$ is the self-inductance of each coil on the delta-delta winding.

The mutual inductance M represents the mutual inductances between the primary side and the secondary side, which contributes to the power transmission, e.g., the mutual inductance between L_{u1A} and L_{u2A}. M_a represents the mutual inductance between the adjacent coils, e.g., the mutual inductance between L_{u1A} and L_{v1B}. The mutual inductance M_b represents the mutual inductance between the coils, which are placed apart from 120 degrees, e.g., the mutual inductance between L_{u1A} and L_{w1A}. The mutual inductance M_c represents the mutual inductance between the opposite coils, e.g., the mutual inductance between L_{u1A} and L_{u1B}. The suffix "1" indicates inductances on the primary side, and "2" means inductances on the secondary side. Note that other unwanted mutual inductances, e.g., the mutual inductance between L_{u1A} and L_{u2B} are ignored in Eq. (1).

It is clear from Eq. (1) that the unwanted mutual inductances cause an unwanted induce voltage on each of the transmission coils. This induced voltage decreases the efficiency due to a circulating current. The canceling method of these unwanted induced voltages will be explained in the next section.

C. Cancellation of Magnetic Interference Coupling

In this section, the canceling method of unwanted induced voltage caused by the magnetic interference is explained. The cancellation method of the magnetic interference coupling is explaind with the star-star winding. However, the cancellation technique can be used for the delta-delta winding.

The induced voltage on L_{u1} is derived from the first column of Eq. (1),

$$\begin{aligned} v_{u1A} = {} & L_{1Ys}\frac{di_{u1}}{dt} + M\frac{di_{u2}}{dt} - M_{c1}\frac{di_{u1}}{dt} \\ & - M_{a1}\left(\frac{di_{v1}}{dt} + \frac{di_{w1}}{dt}\right) + M_{b1}\left(\frac{di_{v1}}{dt} + \frac{di_{w1}}{dt}\right) \end{aligned} \tag{3}$$

The first term of the right side in Eq. (3) is the induced voltage by self-inductance, the second term is the mutual inductance caused by the coil on the secondary side. The second term contributes to the power transmission. The third to fifth terms are the induced voltage caused by the interference coupling. If the third to fifth terms of Eq. (3) is zero, the relationship between the primary coil L_{1Ys} and the secondary coil L_{2Ys} is seen as the same as a transmission with one-by-one.

Assuming the three-phase equilibrium, Eq. (3) is transformed as

$$\begin{aligned} v_{u1A} = {} & L_{1Ys}\frac{di_{u1}}{dt} + M\frac{di_{u2}}{dt} \\ & - \omega I_m\left\{M_{c1}\cos\omega t + \left(M_{a1} - M_{b1}\right)\cos\left(\omega t - \frac{2}{3}\pi\right)\right. \\ & \left. \left(M_{a1} - M_{b1}\right)\cos\left(\omega t - \frac{4}{3}\pi\right)\right\} \end{aligned} \tag{4}$$

where I_m is the maximum value of the primary current i_{u1}, which flows in each of the primary coils.

From Eq. (4), it is found that the unwanted induced voltage does not occur when

$$M_{a1} = M_{b1} + M_{c1} \tag{5}$$

is satisfied.

Because the self-inductance of the primary coils L_{1Ys} is equal to each other, the canceling condition of the unwanted induced voltage is

$$k_{a1} = k_{b1} + k_{c1} \tag{6}.$$

Therefore, the unwanted coupling can be canceled by designing the magnetic coupling according to Eq. (6) on the primary side.

Similarly, the unwanted coupling on the secondary side can be canceled by designing the magnetic coupling according to Eq. (7).

$$k_{a2} = k_{b2} + k_{c2} \tag{7}$$

Figure 4 shows the simulated relationship between the inverter output power factor and the magnetic interference couplings k_a, k_b, and k_c. The dotted line on the graph represents Eq. (6). Fig. 4 (a), (b), and (c) show the relation when the magnetic interference coupling k_b is zero, 0.1 and 0.2, respectively. When the magnetic interference coupling is small enough to be negligible, the power factor closes to unity. The power factor decreases when one of the interference coupling increases. However, the power factor remains at high even when the interference couplings increase under as long as Eq. (6) is satisfied. On the other words, these results show that the magnetic interferences among the transmission coils do not affect the power factor when the relation of the interference coupling fits on Eq. (6).

III. Design of Three-phase IPT System

In this chapter, the design method of proposed three-phase IPT system with the star-tar winding and the delta-delta winding is described. In this design procedure, the induced voltage generated by the magnetic interference among the multiple coils can be ignored with assuming Eq. (6–7).

A. Star-star winding

This section represents the design method of the proposed three-phase IPT system with the star-star winding shown in Fig. 1 (a) with.

1) Equivalent AC resistance

The equivalent AC resistance is calculated from the rated output voltage V_{DC2}, and rated output power P. The equivalent AC resistance R_{eq} can be calculated by expanding a derivation of an equivalent AC resistance of a single-phase rectifier to the three-phase rectifier. The equivalent AC resistance for a certain phase is expressed by

$$R_{eq} = \frac{8}{\pi^2}\frac{\left(V_{DC2}/2\right)^2}{P/3} = \frac{6}{\pi^2}\frac{V_{DC2}^2}{P} \tag{8}.$$

2) Secondary inductance

Maximizing a transmission efficiency, an impedance of the secondary inductance should be equal to the impedance of the equivalent AC resistance. By ignoring a

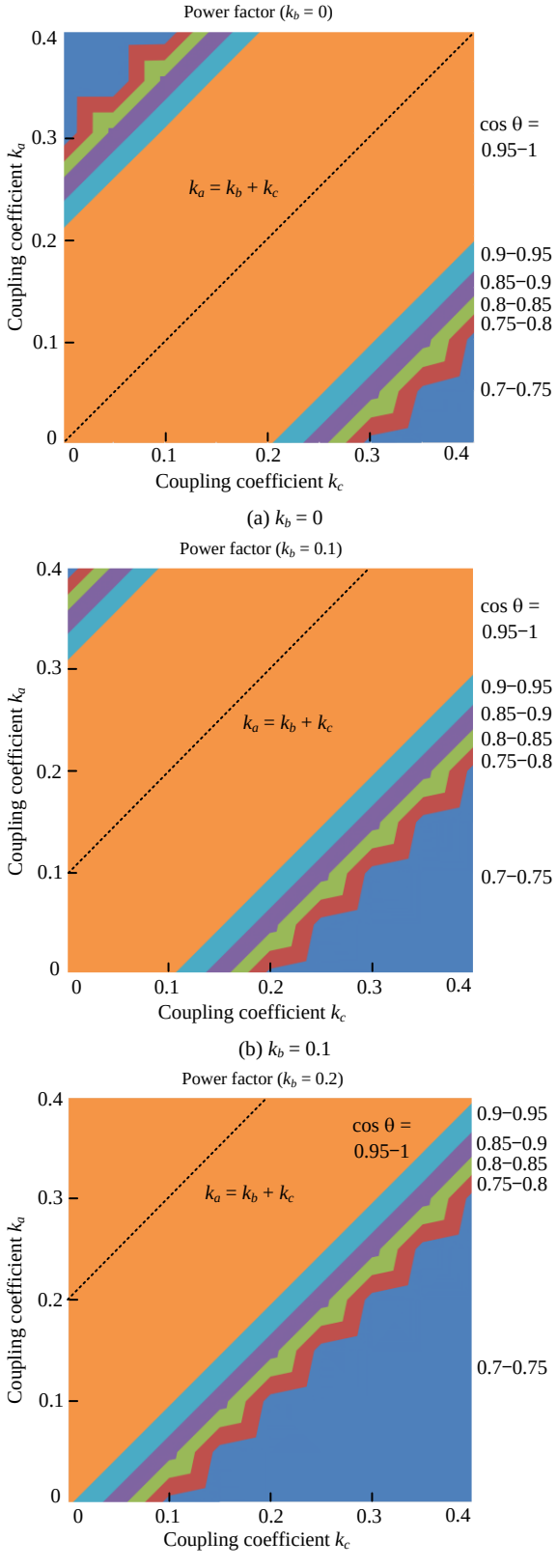

Fig. 4. Effect of magnetic interference coupling on power factor.

winding resistance and assuming the following resonance condition, the secondary self-inductance for a certain phase should be

$$L_{2Y} = L_{u2} = L_{v2} = L_{w2} = \frac{6}{\pi^2 k\omega}\frac{V_{DC2}^2}{P} \quad (9),$$

where ω is the transmission angular frequency, k is the coupling coefficient.

The secondary inductances have to be half because two transmission coils are connected in each phase in the proposed IPT system. Thus, inductance for a certain coil is $L_{2Ys} = L_{2Y}/2$.

3) Primary inductance

From the voltage ratio between the input DC voltage V_{DC1} and the output DC voltage V_{DC2} under the resonance condition, a primary self-inductance for obtaining the desired rated voltage is expressed by

$$L_{1Y} = L_{u1} = L_{v1} = L_{w1} = L_{2Y}\left(\frac{V_{DC1}}{V_{DC2}}\right)^2 = \frac{6}{\pi^2 k\omega}\frac{V_{DC1}^2}{P} \quad (10),$$

where the primary inverter is operated with a square-wave operation. In the proposed IPT system, the transmission coils are divided and connected in series. The inductances represented by Eq. (10) have to be half. Thus, the inductance of primary coil is $L_{1Ys} = L_{1Y}/2$.

4) Resonance capacitors

Besides, the resonance capacitors are connected to the primary inverter and the rectifier in series. The resonance capacitors are designed to resonate with the self-inductance at the transmission angular frequency ω. Thus, the resonant capacitors can be designed as

$$C_{u1Y} = C_{v1Y} = C_{w1Y} = \frac{1}{\omega^2 L_{1Y}} \quad (11),$$

$$C_{u2Y} = C_{v2Y} = C_{w2Y} = \frac{1}{\omega^2 L_{2Y}} \quad (12).$$

Note that, the operating frequency is slightly adjusted to achieve a zero-voltage switching of the MOSFETs in the inverter.

B. Delta-delta winding

This section describes the design method of the proposed three-phase IPT system with the delta-delta winding shown in Fig. 1 (b).

The equivalent resistance for the star connection is as same as the star-star winding.

1) Secondary inductance

The secondary inductance $L_{2\Delta}$ should be equal to the impedance of the equivalent AC resistance. Thus the secondary inductance with a star winding is expressed by

$$L_{2Y} = \frac{R_{eq}}{k\omega} = \frac{6}{\pi^2 k\omega}\frac{V_{DC2}^2}{P} \quad (13)$$

with assuming small winding resistance under the resonance condition.

The secondary inductance expressed by Eq. (13) have be transformed into the inductance for the star-star winding. The secondary inductance is expressed by

$$L_{2\Delta} = L_{uv2} = L_{vw2} = L_{wu2} = 3L_{2Y} = \frac{18}{\pi^2 k\omega}\frac{V_{DC2}^2}{P} \quad (14).$$

The inductance expressed in Eq. (14) have to be half in the proposed IPT system because the transmission coils are divided and connected in series.

2) Primary inductance

The primary inductance is calculated by Eq. (15) from the voltage ratio between the primary DC voltage and the secondary DC voltage when the primary inverter is operated in square-wave operation mode.

$$L_{1\Delta} = L_{uv1} = L_{vw1} = L_{wu1} = L_{2\Delta}\left(\frac{V_{DC1}}{V_{DC2}}\right)^2 = \frac{18}{\pi^2 k\omega}\frac{V_{DC1}^2}{P} \quad (15)$$

The primary inductances also have to be half.

3) Resonance capacitors

The resonance capacitors are connected in series to the output of the inverter and the input of the rectifier. The resonance capacitors are designed to resonate with the primary and the secondary inductance at the transmission angular frequency ω.

$$C_{u1\Delta} = C_{v1\Delta} = C_{w1\Delta} = \frac{3}{\omega^2 L_{1\Delta}} \quad (16)$$

$$C_{u2\Delta} = C_{v2\Delta} = C_{w2\Delta} = \frac{3}{\omega^2 L_{2\Delta}} \quad (17)$$

IV. Experimental Verification

Figure 5 and Table I show the prototype and its specifications. In this paper, the proposed IPT system with the star-star winding is experimentally demonstrated. The magnetic interference couplings are $k_a = 0.048$, $k_b = 0.011$, and $k_c = 0.003$. The each transmission coils have ferrite plates of 245 × 215 × 10 mm. The ferrite plates are put into boxes made from acrylic. As windings for the transmission coils, a litz-wire is used.

Figure 6 shows the operation waveforms with the 3-kW prototype. Fig. 6 (a) shows the inverter output voltage v_{uv1}, output current i_{u1}, rectifier input current i_{u2} and output voltage V_{DC2}. Note that the line voltage v_{uv1} as the inverter output voltage is observed. Thus, the inverter output current lags 30 degrees with respect to the inverter output line-volage. It means that the power factor correction using resonance is achieved despite the magnetic interference coupling. Moreover, it is confirmed that power is transmitted from the primary side to the secondary side.

Figure 7 shows the voltage gain between the primary DC voltage and the secondary DC voltage. The dotted line is the theoretical curve, which is calculated by ignoring the magnetic interference among the coils. The experimental results almost agree with the theoretical curve except for low load region. In the low-load area,

(a) Three-phase inverter

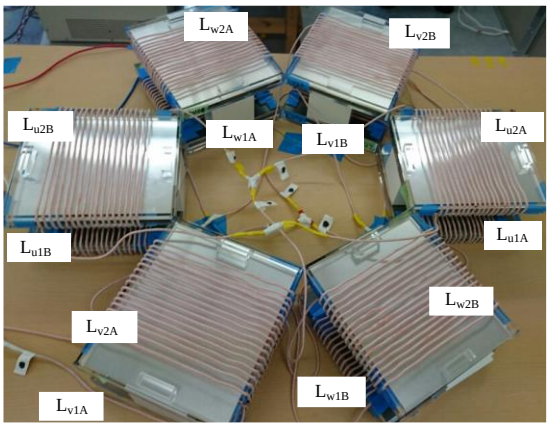

(b) Transmission coils

Fig. 5. 3-kW prototype.

Table 1. Specifications of the prototype.

Item	Symbol	Value	
Primary DC voltage	V_{DC1}	400	V
Secondary DC voltage	V_{DC2}	400	V
Rated power	P	3.0	kW
Transmission frequency	f	85.6	kHz
Coupling coefficient	k	0.26	
	k_a	0.048	
Interference coupling	k_b	0.011	
	k_c	0.003	
Primary inductance	L_{1Ys}	106	uH
Secondary inductance	L_{2Ys}	106	uH
Primary capacitance	C_{u1Y}, C_{v1Y}, C_{w1Y}	16.5	nF
Secondary capacitance	C_{u2Y}, C_{v2Y}, C_{w2Y}	16.5	nF
MOSFETs	SCT3030AL (ROHM)		
Diodes	VS-20ETF06-M3 (Vishay)		

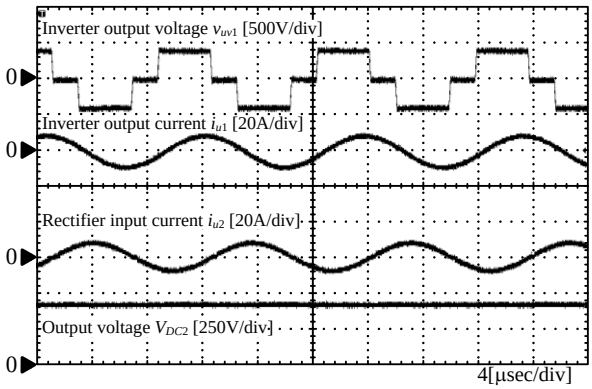

(a) Inverter output voltage, output current, rectifier input current and output voltage

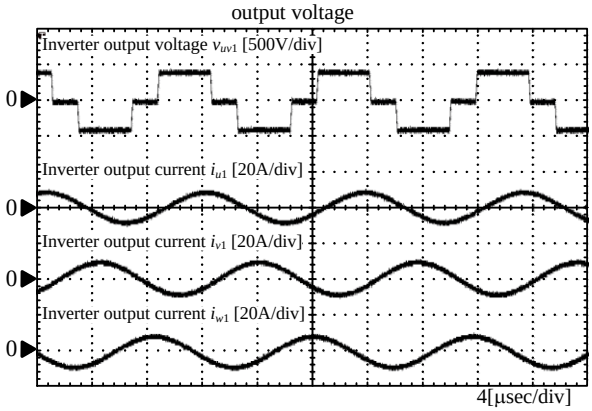

(a) Inverter output voltage and output currents on the primary side

Fig. 6. Operation waveforms.

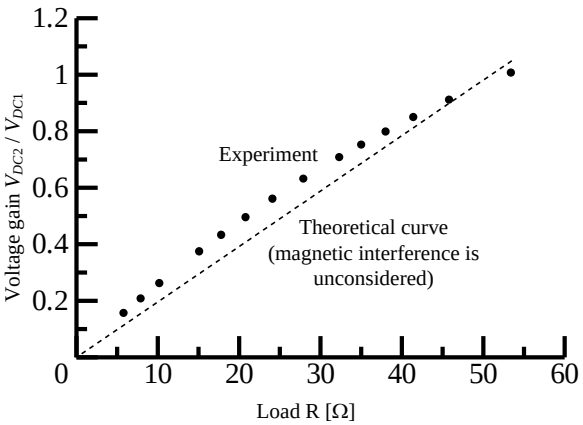

Fig. 7. Voltage gain between primary voltage and secondary voltage.

the hard switching occurs because the current during the dead time is not enough to achieve zero-voltage switching. Due to the hard switching, the voltage gain is slightly different to the theoretical curve.

Figure 8 shows the measured efficiency characteristic from the primary DC voltage to the secondary DC voltage. In fact, the efficiency takes into account the power loss in the inverter and the rectifier. The maximum efficiency reaches 91%. The reason why the efficiency is not so high because the transmission coils of the prototype are a scaled-down model. Thus, the efficiency is expected to be improved in an actual application.

Figure 9 shows the measuring point of the radiation noise. The radiation noise is measured at 2 m from the coil edge. The radiation noise is measured in a shielded room. As the conventional system, three-phase IPT system with three coils is tested for the comparison on the radiation noise. When the conventional method is tested, the six coils (coil B in Fig. 2) are removed. The transmission coils of phase-v and phase-w are placed in an angle of 120 degrees to the coils on phase-u.

Moreover, the radiation noise is compared under the same current condition. In order to remove the effect of the radiation noise from the inverter, the inverter is placed out of the shield room.

Figure 10 shows the radiation noise. Fig. 10 (a) is the radiation noise generated by the conventional three-phase IPT system with six coils where the coils B in Fig. 2 are

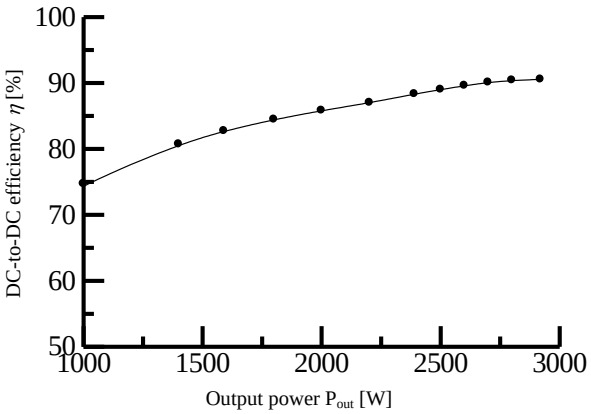

Fig. 8. Efficiency characteristic.

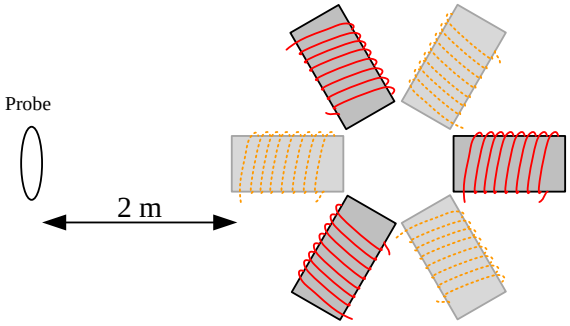

(a) For conventional three-phase IPT system

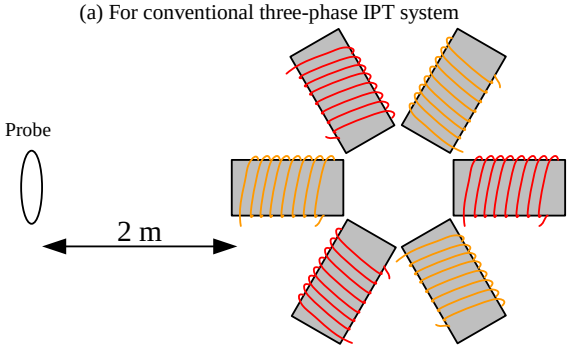

(b) For proposed three-phase IPT system

Fig. 9. Measurement of radiation noise.

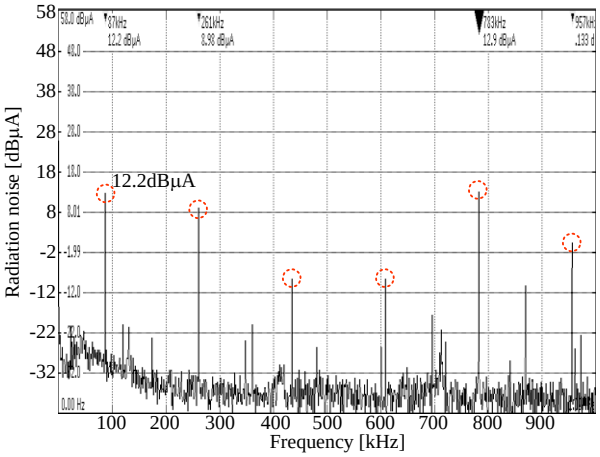

(a) Conventional three-phase IPT system with six coils.

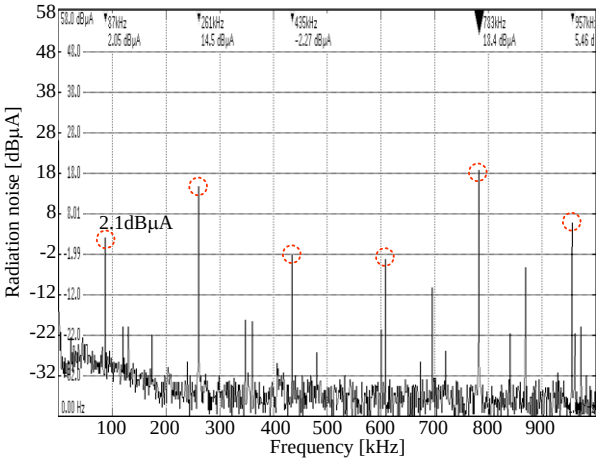

(a) Proposed three-phase IPT system with 12 coils.

Fig. 10. Radiation noise at 2 m from the coil edge.

removed. Fig. 10 (b) is the radiation noise generated by the proposed IPT system with 12 coils. The measurement distance and conditions are same as those in Fig. 10 (a). In both the experiments, common transmission coils are used. In order to have a fair comparison, the conduction currents on each coil are adjusted to be same by adjusting the input DC voltage. Note that the inverter and the rectifier are put outside of the shielded room in order to measure only the radiation noise from the transmission coils.

The radiation noise at the fundamental frequency is suppressed from 12.2dBμA to 2.1dBμA by the proposed IPT system. It is confirmed that the proposed three-phase IPT system is effective to reduce the fundamental radiation noise. However, the radiation noise on the third-order harmonics of the proposed system slightly increases.

V. CONCLUSION

This paper proposed three-phase inductive power transfer system. The proposed system has six primary coils and six secondary coils. The opposite coils, which are in series and are differentially connected, cancel out the radiation noise. Moreover, the six coils on each side allow to cancel out the magnetic interference among the multiple coils. Due to the cancel of the magnetic interference, the IPT system can be operated with an unity power factor regarding the inverter output.

In this paper, the effect of the magnetic interference and its cancellation method is mathematically introduced. Then, the proposed scaled-mode was experimentally tested with the 3-kW prototype. The experimental results shows that the maximum DC-to-DC efficiency is 91%. Finally, the radiation noise is evaluated and compared to the conventional three-phase IPT system with six coils. The proposed method suppresses the radiation noise, which is measured at 2 m from the coil edge, from 12.2dBμA to 2.1dBμA on the fundamental frequency.

REFERENCES

[1] A. Kurs, R. Moffatt, M. Soljacic, "Simultaneous mid-range power transfer to multiple devices," *Applied Physics Letters*, No. 044102, pp. 96-98 (2009)

[2] A. Kurs, A. Karalis, R. Moffatt, J. D. Joannopoulos, P. Fisher, and M. Soljacic, "Wireless Power Transfer via Strongly Coupled Magnetic Resonances," *Science*, Vol. 317, pp. 83-86 (2007)

[3] S. Weearsinghe, D. J. Thrimawithana, and U. K. Madawala, "Modeling Bidirectional Contactless Grid Interfaces With a Soft DC-Link," *IEEE Trans. On Power Electronics*, Vol. 30, No. 7, pp. 3528-3541 (2015)
[4] F. Y. Lin, G. A. Covic, and J. T. Boys, "Evaluation of Magnetic Pad Sizes and Topologies for Electric Vehicle Charging," *IEEE Trans. On Power Electronics*, Vol. 30, No. 11, pp. 6391-6407 (2015)
[5] M. Budhia, J. T. Boys, G. A. Covic, and C. Huang, "Development of a Single-Sided Flux Magnetic Coupler for Electric Vehicle IPT Charging Systems," *IEEE Trans. On Industrial Electronics*, Vol. 60, No. 1, pp. 318-328 (2013)
[6] C. Huang, J. T. Boys, and G. A. Covic, "LCL pickup Circulating Current Controller for Inductive Power Transfer Systems," *IEEE Trans. On Power Electronics*, Vol. 28, No. 4, pp. 2081-2093 (2013)
[7] T. Koyama, K. Umetani, and E. Hiraki, "Design Optimization Method for the Load Impedance to Maximize the Output Power in Dual Transmitting Resonator Wireless Power Transfer System," *IEEJ Journal of Industry Applications*, Vol. 7, No. 1, pp. 49-55 (2018)
[8] T. Yamamoto, Y. Bu, T. Mizuno, Y. Yamaguchi, and T. Kano, "Loss Reduction of Transformer for LLC Resonant Converter Using a Magnetoplated Wire," *IEEJ Journal of Industry Applications*, Vol. 7, No. 1, pp. 43-48 (2018)
[9] G. lovison, D. Kobayashi, M. Sato, T. Imura, and Y. Hori, "Secondary-side-only Control for High Efficiency and Desired Power with Two Converters in Wireless Power Transfer Systems," *IEEJ Journal of Industry Applications*, Vol. 6, No. 6, pp. 473-481 (2017)
[10] K. Kusaka. J. Itoh, "Development Trends of Inductive Power Transfer Systems Utilizing Electromagnetic Induction with Focus on Transmission Frequency and Transmission Power," *IEEJ Journal of Industry Applications*, Vol. 6, No. 5, pp. 328-339 (2017)
[11] R. Ota, N. Hoshi, and J. Haruna, "Design of Compensation Capacitor in S/P Topology of Inductive Power Transfer System with Buck or Boost Converter on Secondary Side," *IEEJ Journal of Industry Applications*, Vol. 4, No. 4, pp. 476-485 (2015)
[12] International Organization for Standardization, "Electrically propelled road vehicles — Magnetic field wireless power transfer — Safety and interoperability requirements," Publicly available specification: ISO/PAS19363:2017(E)
[13] International Electrotechnical Commission, "Electric vehicle wireless power transfer (WPT) systems – Part 1: General requirements," International standard: IEC 61980-1 (2015)
[14] T. Shijo, K. Ogawa, M. Suzuki, Y. Kanekiyo, M. Ishida, and S. Obayashi, "EMI Reduction Technology in 85 kHz Band 44 kW Wireless Power Transfer System for Rapid Contactless Charging of Electric Bus," *IEEE Energy Conversion Congress & Expo 2016*, No. EC-0641 (2016)
[15] M. Suzuki, K. Ogawa, F. Moritsuka, T. Shijo, H. Ishihara, Y. Kanekiyo, K. Ogura, S. Obayashi, and M. Ishida, "Design method for low radiated emission of 85 kHz band 44 kW rapid charger for electric bus," *IEEE Applied Power Electronics Conference and Exposition 2017*, pp. 3695-3701 (2017)
[16] T. Shijo, K. Ogawa, F. Moritsuka, M. Suzuki, H. Ishihara, Y. Kanekiyo, K. Ogura, M. Ishida, S. Obayashi, S. Shimmyo, K. Maki, F. Takeuchi, and N. Tada, "85 kHz band 44 kW wireless power transfer system for rapid contactless charging of electric bus," *International Symposium on Antennas and Propagation 2016*, pp. 38-39 (2016)
[17] D. J. Thrimawithana, U. K. Madawala, A. Francis, and M. Neath: "Magnetic Modeling of a High-Power Three Phase Bi-Directional IPT System," *37th Annual Conference of the IEEE Industrial Electronics Society*, pp. 1414-1419 (2011)
[18] G. A. Covic, J. T. Boys, M. L. G. Kissin, and H. G. Lu: "A Three-Phase Inductive Power Transfer System for Roadway-Powered Vehicles," *IEEE Trans. on Industrial Electronics*, Vol. 54, No. 6, pp. 3370-3378 (2007)
[19] A. Laka, J. A. Barrena, J. Chivite-Zabalza, M. A. Rodriguez, and P. Izurza-Moreno: "Isolated Double-Twin VSC Topology Using Three-Phase IPTs for High-Power Applications," *IEEE Trans. on Power Electronics*, Vol. 29, No. 11, pp. 5761- 5769 (2014)
[20] M. Kim, S. Ahn, and H. Kim: "Magnetic Design of a Three-Phase Wireless Power Transfer System for EMF Reduction," *IEEE Conference on Wireless Power Transfer Conference 2014*, pp. 17-20 (2014)
[21] Y. H. Sohn, B. H. Choi, E. S. Lee, G. C. Lim, G. Cho, and C. T. Rim: "General Unified Analyses of Two-Capacitor Inductive Power Transfer Systems: Equivalence of Current-Source SS and SP Compensations," *IEEE Trans. On Power Electronics*, Vol. 30, No. 11, pp. 6030-6045 (2015)
[22] International Special Committee on Radio Interference, "Industrial, scientific and medical equipment — Radio-frequency disturbance characteristics — Limits and methods of measurement," CISPR 11: 2015 (2015)